Ultrasonic Longitudinal-Wave Attenuation in Superconducting Mercury*

H. C. Wu, † H. V. Bohm, and R. L. Thomas

Department of Physics, Wayne State University, Detroit, Michigan 48202

(Received 12 December 1969)

This paper presents results of measurements of the attenuation of longitudinal-wave ultrasound in pure single crystals of mercury in both the normal and superconducting states. Measurements were made for frequencies from 10 to 320 MHz and for three different crystallographic directions of sound propagation. A distinct frequency-dependent behavior was observed, and is consistent with a state-dependent electron mean free path. Tests for dislocation damping mechanisms in the background attenuation were negative: No amplitude dependence was observed over a 60-dB dynamic range, and reasonable fits to the frequency and field dependence of the data at various temperatures were made, using free-electron theory. An anomalous behavior persists in the high-frequency limit which cannot be explained in terms of a single-energy-gap BCS theory.

I. INTRODUCTION

In an earlier publication,[1] the authors reported preliminary results of ultrasonic longitudinal-wave attenuation measurements in pure single-crystal specimens of mercury, both in the superconducting state and in the presence of a transverse critical magnetic field. The results reported exhibited substantial qualitative deviations from the Bardeen, Cooper, and Schrieffer (BCS) theory,[2] which predicts that the ratio of the electronic attenuation in the superconducting state (α_s) to that in the normal state (α_n) is given by

$$\alpha_s / \alpha_n = 2/(1 + e^{\Delta(T)/kT}) , \qquad (1)$$

where $\Delta(T)$ is the temperature-dependent superconducting energy gap. There are two main features of the apparently anomalous data: (a) a marked frequency dependence with a limiting behavior in the high-frequency limit, $ql \gg 1$, where q represents the ultrasonic wave number, and l represents the electron mean free path; (b) in the case of limiting behavior, the attenuation drop just below the critical temperature is much more rapid than that predicted by the BCS theory and is considerably more gradual than the BCS prediction for low-reduced temperatures. Similar qualitative behavior has since been reported by Newcomb and Shaw,[3] hereafter referred to as NS, who made independent measurements on pure single-crystal mercury.

Measurements of ultrasonic attenuation in other superconductors, both strong[4-6] and weak coupling[7,8] have also exhibited departures from BCS behavior. In the case of tin, for which earlier ultrasonic measurements[9] had established a strongly anisotropic-effective energy-gap parameter, Claiborne and Einspruch[7] have had some success in explaining the departures in terms of this

anisotropy, together with the assumption of multiple gaps associated with the energy surfaces in the higher Brillouin zones. Newcomb and Shaw[3] have also applied this phenomenological two-gap model to mercury-cadmium single-crystal alloys. Applying this procedure to the present pure mercury data yields extreme values for the two gaps. An alternative explanation of the sharp drop near T_c advanced by Dobbs and Thomas,[8] uses the real metal modification of Eq. (1) which was given by Perz.[10] In this approach, Eq. (1) is modified by a factor $J_1/(J_1 + J_2)$, in the limit $ql \gg 1$, where J_1 is an integral over an effective zone on the Fermi surface of angular width $1/ql$, and J_2 is an integral over the entire Fermi surface. Only for longitudinal waves propagated along a sufficiently high-symmetry axis does $J_2 = 0$. For lower-symmetry sound propagation, or for quasilongitudinal modes slightly off axis, a rapid drop is expected just below T_c. In contradiction to the present mercury results, however, this mechanism does not predict a limiting behavior for $ql \gg 1$, but rather an increasingly sharp drop near T_c.

Not all of the ultrasonic measurements in pure mercury have exhibited the anomalies described above. Ferguson and Burgess[11] made measurements of ultrasonic attenuation in thin specimens (3×10^{-3} cm) of polycrystalline mercury at 9 GHz, and found good agreement with Eq. (1), assuming a zero-temperature gap of $2\Delta(0) = 4.0kT_c$. They suggest that a temperature-dependent dislocation damping[12] may account for the anomalies observed at lower ultrasonic frequencies. Such mechanisms generally have been acknowledged to play an important role in ultrasonic measurements in superconductors, the most pathological case being lead. In the most recent measurements on lead by Fate *et al.*,[6] the pronounced dependence of the attenuation behavior upon driving amplitude was confirmed, al-

though an anomalous behavior was found to persist even in the low-amplitude limit. Furthermore, the normal-state data in lead in this limit were found to be in reasonable agreement with free-electron theory,[13] suggesting that dislocation damping which varies with temperature and frequency, but is independent of driving amplitude,[12] is also unlikely to be the source of the anomalous behavior for that metal. The results of similar investigations in mercury will be described in this paper.

Although the original BCS theory assumes weak coupling as well as the condition $ql \gg 1$, subsequent calculations have been made[14-17] which relax both of these assumptions. The present mercury data, however, are in disagreement with the results of the strong coupling calculations, which reduce to Eq. (1) in the limit $ql \gg 1$, and predict departures from Eq. (1) near T_c when $ql \ll 1$. The ql dependence of these theoretical predictions, attributed to a state-dependent electron mean free path, find qualitative experimental support in the work of Fate et al.,[6] although only for the temperature region near T_c. The results of the present investigation suggest that the concept of an electron mean free path which differs in the normal and superconducting states could also explain the observed frequency-dependent behavior in mercury within the framework of the free-electron model. The striking difference, however, is that for mercury the anomalous behavior remains in the limit $ql \gg 1$.

II. TECHNIQUE

Measurements were made on samples of dimensions $1\frac{1}{2}$ in. $\times \frac{1}{2}$ in. $\times \frac{1}{16}$ in. having plane, parallel faces oriented to within five degrees of being normal to a [111], [$\bar{1}$10], or [$3\bar{1}\bar{1}$] crystallographic axis, prepared from 99.9999% purity mercury supplied by the United Mineral and Chemical Co. A detailed description of the procedures used in preparing the oriented single crystals of mercury for this work has been reported elsewhere.[18]

The ultrasonic measurements were carried out using the conventional pulse-echo technique,[19] single transducer or transmission methods. Because of the thinness of the samples, an X-cut quartz delay rod was employed with 10-MHz resonant frequency X-cut transducers. A successful bonding agent for these samples was found to be GC Pliobond cement.[20]

A block diagram of the electronics is shown in Fig. 1. For the low-frequency (< 200-MHz) measurements, a Sperry Product Ultrasonic Attenuation Comparator served as both the transmitter and superheterodyne receiver. Because of the somewhat high noise figure of this instrument, a narrow-band rf preamplifier was usually employed over this frequency range to provide approx-
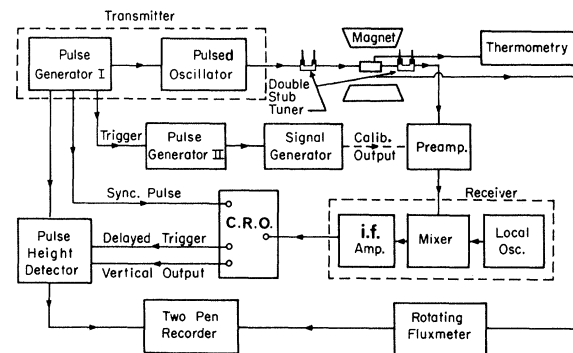

FIG. 1. Block diagram of ultrasonic pulse-echo apparatus.

imately 20 dB of additional useful receiver gain. An Arenberg Ultrasonic Laboratory PA-620-B preamplifier was used for this purpose at frequencies up to 50 MHz, supplemented at 50 MHz by an Ameco PV-50 nuvistor preamplifier. A narrowband rf preamplifier was constructed for measurements at 150 MHz and higher. An Applied Microwave Laboratory Model PV5K pulsed oscillator was employed as the transmitter and the Sperry receiver was replaced for frequencies above 230 MHz by a receiver consisting of an LEL Model 4-6235 Converter, a General Radio Co. Model 1209-C local oscillator, and an LEL model 1753-22 i.f. amplifier. In all receiver configurations, the detected output of the i.f. amplifier was displayed on a Tektronix 545 B Oscilloscope whose vertical output was fed to a pulse-height detector,[21] which developed a signal suitable for display on a strip chart recorder. Double stub tuners were used for impedance matching at the higher frequencies. A calibration curve for relative attenuation measurements was made at each frequency, using the pulsed output and calibrated attenuator of a Hewlett-Parkard Model 608C signal generator tuned to the receiver frequency, as shown in Fig. 1.

Sample temperature was monitored by a 47-Ω, $\frac{1}{2}$-W Allen-Bradley carbon resistor which was calibrated against the helium vapor pressure by computer fit to the empirical equation of Clement and Quinnel.[22] The resistor and sample both were in good thermal contact with a brass electrical ground plate, and point-by-point measurements were taken of α_s and α_n with the sample holder in thermal equilibrium with the helium bath as the temperature was lowered. The data were checked for consistency by making similar measurements slowly but continuously on warming. The normal-state attenuation was measured by applying an external magnetic field normal to the direction of sound propagation. In most cases, the sample holder was held continuously at helium temperatures un-

til data had been taken for several different frequencies, so as to use the same thermometer calibration and to maintain similar sources of background attenuation for the sample under investigation.

In order to compare experimental data with the BCS predicted behavior of Eq. (1), it is first necessary to subtract any background attenuation which is of nonelectronic origin. Conventionally this is done simply by extrapolating the observed attenuation in the superconducting state to $T = 0$ where α_s (electronic) $= 0$. The remaining attenuation is then usually assumed to be temperature independent and experimental values of α_s and α_n are measured relative to this extrapolated background attenuation. Such a smooth extrapolation was made in analyzing the present data, and because of the high critical temperature of mercury the correction term is small. However, the possibility of temperature-independent dislocation damping requires that experimental justification be made for the assumption that the background attenuation is constant.

In analyzing the attenuation data in the normal state, taken in the presence of a transverse external magnetic field greater than the critical magnetic field H_c, a further extrapolation must be made to determine what the normal-state attenuation would be in the absence of the magnetic field. Typical field-dependence plots of the normal-state attenuation over the range from H_c to 12 kG are shown in Fig. 2. The zero-field correction is small for temperatures above 2.2 °K, and although below this temperature the extrapolation is hampered by the presence of magnoacoustic oscillations, in that temperature range the total attenuation is also largest. The maximum extrapolation error at the lowest temperatures is estimated to be 5%.
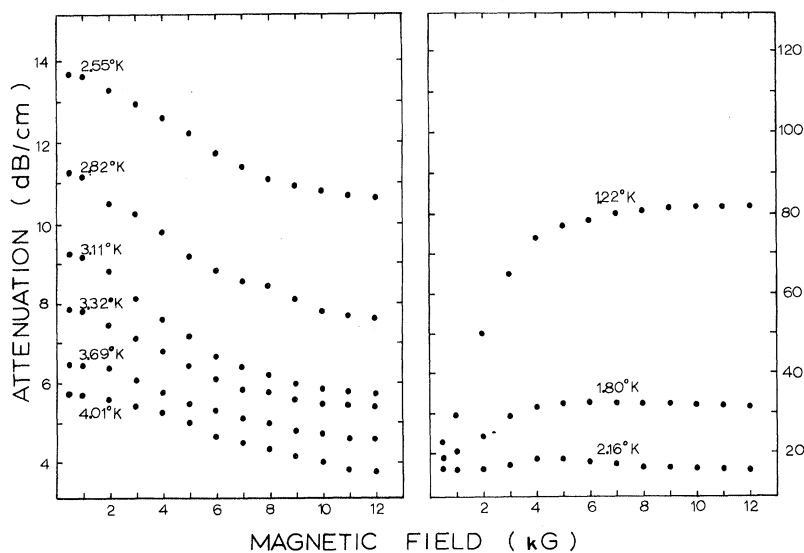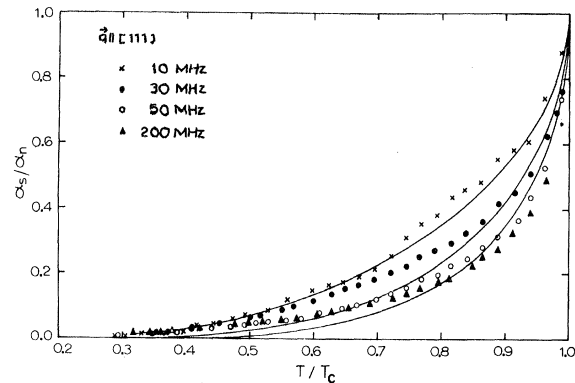

FIG. 3. Temperature dependence of the normalized logitudinal-wave ultrasonic attenuation for propagation along [111]. The upper, middle, and lower solid curves are BCS theory results for $2\Delta(0) = 3.5kT_c$, $4.6kT_c$, and $5.4kT_c$, respectively.

III. RESULTS

Representative experimental plots are given in Figs. 3–5 for sound propagation along the [111], [$\bar{1}$10], and [$3\bar{1}\bar{1}$] crystallographic directions, respectively. For the purpose of clarity, other data which were taken at i.f. are not plotted. In addition, it should be pointed out that data taken on a second [$3\bar{1}\bar{1}$] crystal at frequencies between 155 and 320 MHz were within experimental scatter of the 155-MHz curve shown in Fig. 5.

The qualitative features of the frequency-dependent results illustrated in Figs. 3–5 were also evident in the data of NS. The latter exhibited the same monotonically increasing rate of falloff near T_c for sound frequencies up to 130 MHz. For a larger range of frequencies from 10 to 320 MHz, the results of the present work indicate that a
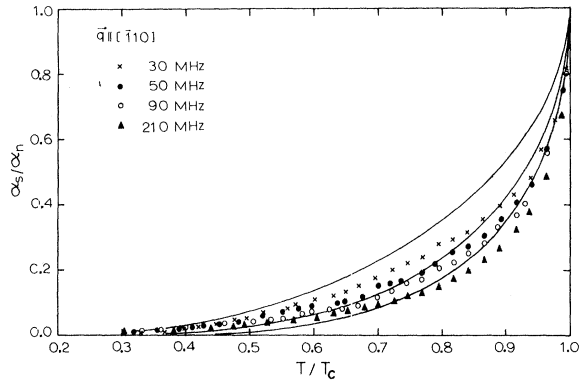

FIG. 2. Isothermal field dependence of α_n at 50 MHz with $q \parallel$ [111].

MAGNETIC FIELD (kG)

FIG. 4. Data for $\vec{q} \parallel [\bar{1}10]$, plotted as in Fig. 3.

limiting behavior is present in all data taken above 150 MHz. Furthermore, in disagreement with the NS results, the limiting behavior shown in Figs. 3–5 indicates that no effective energy-gap anisotropy is detectable in the present data within experimental scatter. This may not be a meaningful discrepancy with NS, however, since the NS data for propagation along the threefold symmetry direction were severely limited by poor transducer bonds.

As an alternative way of displaying the results for the high-frequency-limiting case, we note that Eq. (1) may be rewritten in the form

$$2 \ln \frac{2\alpha_n}{\alpha_s} - 1 \frac{2\Delta(0)/kT_c}{[\Delta(T)/\Delta(0)](T_c/T)} . \qquad (2)$$

Within the framework of the BCS theory, $[\Delta(T)/\Delta(0)]$ is a universal function, which has been tabulated by Muhlschlegel.[23] A plot of $2\ln(2\alpha_n/\alpha_s - 1)$ versus $\{[\Delta(T)/\Delta(0)](T_c/T)\}$ should therefore be linear with a slope which gives the limiting energy gap, $[2\Delta(0)/kT_c]$. Such a plot for these data is shown in Fig. 6. As was evident from Figs. 3–5, such a single-gap fit is not consistent with the data. The 155-MHz $[3\bar{1}\bar{1}]$ data shown in Fig. 6 were also numerically fitted to a two-gap model:
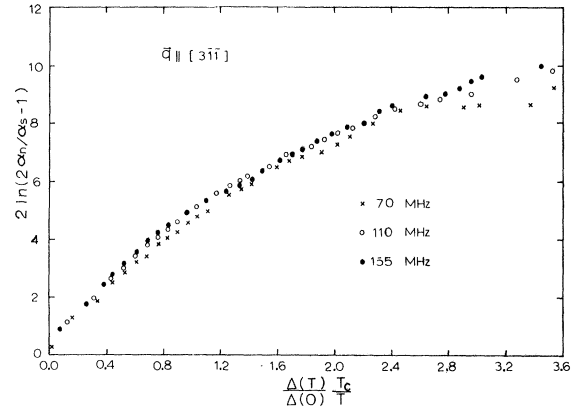

FIG. 6. Data for $\vec{q} \parallel [3\bar{1}\bar{1}]$, replotted according to Eq. (2). See text for results of a numerical two-gap fit to the 155-MHz points.

$$\alpha_s/\alpha_n = A\{1 + \exp[\Delta_1(T)/kT]\}^{-1}$$
$$+ (2 - A)\{1 + \exp[\Delta_2(T)/kT]\}^{-1} , \qquad (3)$$

yielding $A = 1.66$, $2\Delta_1(0) = 7.2kT_c$, and $2\Delta_2(0) = 1.8kT_c$. These values are to be compared with the values of $6.8kT_c$ and $2.6kT_c$ found by NS for 0.01% cadmium-doped twofold symmetry mercury crystals.

IV. EXPERIMENTAL TESTS FOR VARIABLE BACKGROUND ATTENUATION

A careful search for an amplitude-dependent background attenuation was made at two different frequencies. Several complete temperature runs were made on a threefold sample for different relative transducer voltages and frequencies. Representative data taken at 157 MHz are displayed in Fig. 7 with scatter which is within the estimated experimental uncertainty. Similar results were obtained at 50 MHz over an amplitude range of 40 dB. In addition, isothermal measurements were made at 50 MHz of the quantity $(\alpha_n - \alpha_s)$, utilizing the
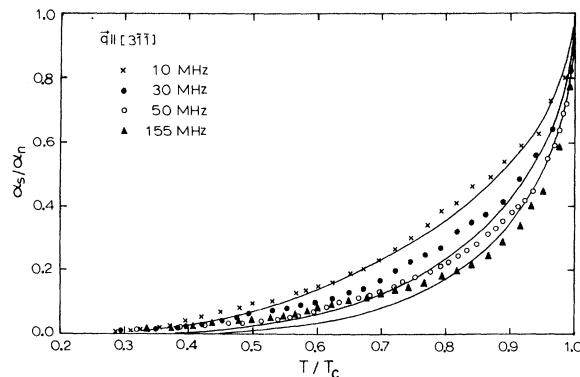

FIG. 5. Data for $\vec{q} \parallel [3\bar{1}\bar{1}]$, plotted as in Fig. 3.
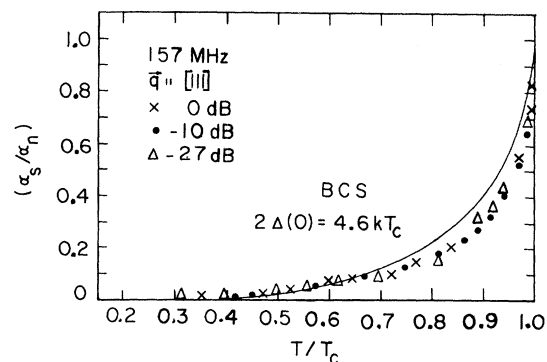

FIG. 7. Test for amplitude dependence as a function of temperature at 157 MHz, $\vec{q} \parallel [111]$.
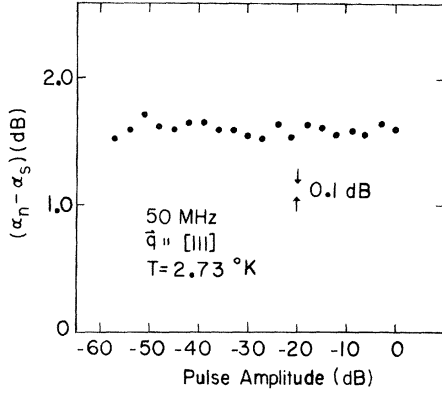
FIG. 8. Isothermal amplitude-dependence test at 50
MHz, $\vec{q} \parallel$ [111].

maximum instrumental dynamic amplitude range of
nearly 60 dB. These data, presented in Fig. 8, al-
so exhibit no discernible amplitude dependence.

If a frequency-dependent source of attenuation of
nonelectronic origin were present, it would be un-
likely that the experimental data would fit Pippard's
calculation[13] which estimates only the conduction
electron contribution to the ultrasonic attenuation:

$$\alpha(ql) = \alpha(\infty) F(ql) \, , \tag{4}$$

where $\alpha(\infty)$, the zero-field attenuation in the limit
$ql \to \infty$, is

$$\alpha(\infty) = (\pi/12) \left(N m v_F \omega / \rho v_L^2 \right) \, ,$$

$$F(q) = \frac{6}{\pi ql} \left(\frac{1}{3} \frac{q^2 l^2 \tan^{-1}(ql)}{ql - \tan^{-1}(ql)} - 1 \right) \, . \tag{5}$$

Here, N is the carrier density, m is the electron
mass, v_L is the longitudinal sound velocity, ρ is
the metal density, and ω is the angular sound fre-
quency. Hence, as a further test for sources of
ultrasonic attenuation other than the conduction
electron system, the experimental data were fitted
to Eq. (4) at several different temperatures and
frequencies. The value of the quantity $\alpha(\infty)/\omega$ was
determined initially by fitting the frequency-depen-
dent data at 2.0 °K to Eq. (4). At other tempera-
tures, l was determined as a single adjustable fit-
ting parameter. The reasonably good fit which was
achieved is illustrated in Fig. 9. Another free-
electron prediction[13] which was verified for these
data is that $\alpha_n(H) \sim H^{-2}$ in the limit of large trans-
verse magnetic fields. This relation was found to
hold over the experimental temperature range.

An independent procedure was used to test the
reliability of the above method for estimating the
electron mean free path as a function of tempera-
ture. Deaton and Gavenda,[24] making numerical
calculations of Pippard's[13] free-electron expres-
sions for longitudinal-wave ultrasonic attenuation,
find that for $ql = 6.8$,

$$\lim \alpha(H, ql) = \alpha(0, ql), \quad \text{as } H \to \infty \, . \tag{6}$$

Experimental data for a given frequency were
taken as a function of magnetic field strength trans-
verse to the direction of propagation (see Fig. 2),
and were extrapolated to the limit of infinite field,
assuming a $1/H^2$ functional dependence for large
values of H. Comparing the measured values of
$\alpha(0, ql)$ and the extrapolated values for $\alpha(\infty, ql)$ to
Eq. (4), $l(T)$ was determined for the normal state
of mercury. As was mentioned previously, $\alpha(0,
ql)$ is similarly obtained by extrapolation from the
measured values near H_c. The functional tempera-
ture dependence of the electron mean free path ob-
tained from the two methods is the same. However,
the latter method yields values of $l(T)$ which are
approximately a factor of 2 larger than those ob-
tained by fitting the zero-field data to Eq. (4).
This is not thought to represent a serious discrep-
ancy, however, in light of the possible effects of
open orbits and other real metal effects on the
high-field-limiting attenuation.[25] In what is possi-
bly another manifestation of such real metal ef-
fects, the infinite-field attenuation, which accord-
ing to the free-electron model should vary as q^2,
was observed to vary approximately as $q^{1.5}$ in
these measurements on mercury.

In comparing the experimental ql dependence
with the free-electron theory as discussed above,
it was also observed that the frequency dependence
of α_s differed systematically from that of α_n at in-
termediate values of reduced temperature, as can
be seen by comparing slopes of log-log plots of
such data shown in Fig. 10. Note that for temper-
atures below 2.5 °K (see Fig. 10), both the normal-
state data (open symbols) and the superconducting
data (closed symbols) yield unity slopes, appro-
priate to the limit $ql \gg 1$, as given by Eq. (4). All
the normal-state data for temperatures higher than
2.5 °K exhibit a nonlinear behavior which is char-
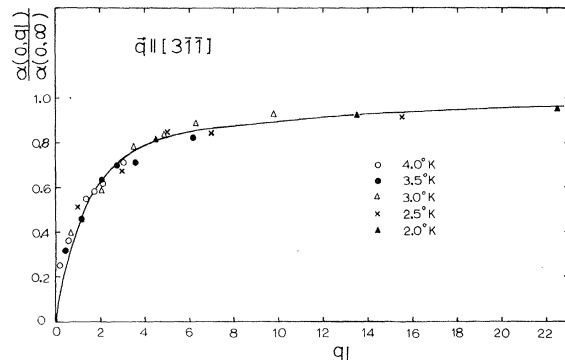acteristic of intermediate ql values, whereas the

FIG. 9. Comparison of experimental $\alpha(0, ql)$ data for
$\vec{q} \parallel$ [3$\bar{1}\bar{1}$] with the free-electron theory, Eq. (4).
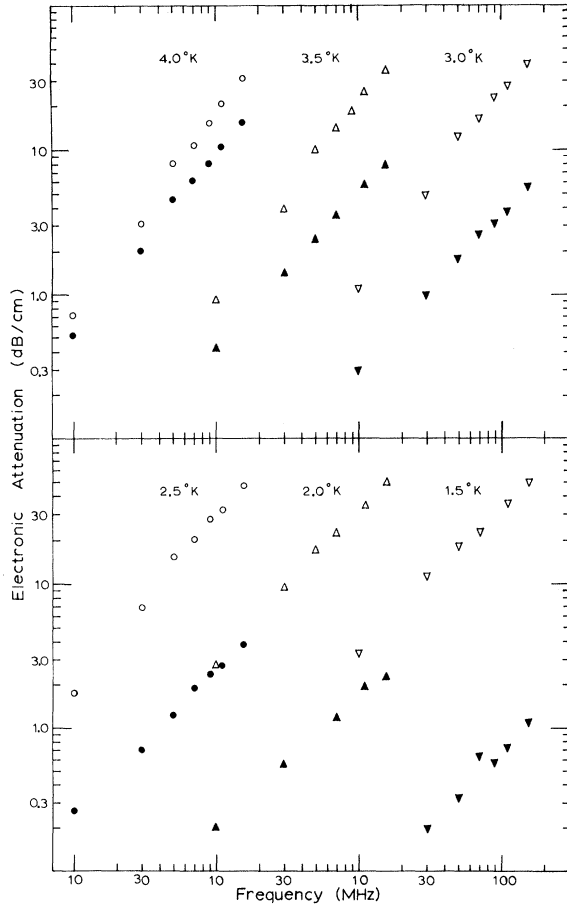
FIG. 10. Log-log plots of the frequency dependence of the attenuation for $\vec{q} \parallel [3\bar{1}\bar{1}]$, both in the normal state (open symbols) and in the superconducting state (closed symbols). For clarity, data at several temperatures have been arbitrarily displaced along the abscissa.

superconducting data only begin to show this behavior at the highest temperature plotted, 4.0 °K. These results strongly suggest that for $T < T_c$, the electron mean free path in the superconducting state is greater than that in the normal state ($l_s > l_n$). This conjecture is also consistent with the frequency dependence displayed in Figs. 3–5, and in particular with the limiting behavior at high frequencies. Evaluating the frequency dependency of the experimental data in terms of Eq. (4) (see Fig. 9), ql_n was found to vary from 0.2 to 4.5 as a function of temperature below T_c at a fixed frequency of 10 MHz, and from 3 to 70 at 155 MHz. Hence, for frequencies above 150 MHz the condition $ql \gg 1$ will be reasonably well satisfied over the whole temperature range below T_c, and any anomalous behavior based upon the fact that $l_s > l_n$ will wash out, since both α_s and α_n are independent of l in this limit. For $ql < 1$, following an approach suggested by Fate,[6] we may rewrite Eq. (1) in the form

$$\alpha_s/\alpha_n = [F(ql_s)/F(ql_n)] f(T) , \qquad (7)$$

where $f(T)$ normally would represent twice the Fermi function of argument $\Delta(T)/kT$, so as to be in agreement with Eq. (1) in the limits $ql_s \gg 1$, $ql_n \gg 1$. For purposes of discussing the present *anomalous* data, $f(T)$ will be assumed simply to be an unknown functional temperature dependence which may be more appropriate for mercury. If $l_s > l_n$ for mercury, as the isothermal frequency-dependent behavior seems to suggest (see Fig. 10), then $F(ql_s)/F(ql_n) > 1$ for $ql < 1$, and α_s/α_n should deviate to values greater than $f(T)$ in this region, in qualitative agreement with the behavior displayed in Figs. 3–5.

V. SUMMARY AND DISCUSSION

The experimental results of the present work, together with those of Newcomb and Shaw,[3] indicate that the temperature dependence of the ultrasonic attenuation departs significantly from the BCS predicted behavior for pure single-crystal mercury. Unlike the NS results for pure mercury, however, the present work indicates very little anisotropy as well as a high-frequency-limiting form which is qualitatively consistent with the assumption that $l_s > l_n$. Although a similar approach has been used by Fate *et al.*[6] to explain ultrasonic measurements in lead in terms of strong coupling theoretical calculations,[15–17] in the case of lead the analysis suggested that $l_n > l_s$, and consequently a frequency dependence which approaches the BCS predicted behavior for large values of ql. Our results for mercury are thus in disagreement with this theory for $ql \gg 1$.

One possible explanation of the deviation from BCS behavior which persists for $ql \gg 1$ is that of multiple energy gaps. A three-adjustable-parameter two-gap numerical fit to the data was attempted. Large differences between the average values of the two gaps are required to fit the data. A possible source of the rapid drop near T_c is that of mixed sound modes because of slight misoriented samples.[8,10] It should be noted, however, that essentially the same limiting behavior was observed for three different orientations. Furthermore, the low-temperature gap of $2\Delta(0) < 2kT_c$ for all orientations is exceedingly small for this strong coupling superconductor. If one compares the behavior in lead,[6] one finds a similar behavior in the limiting case, with $2\Delta(0) < 1.86kT_c$ and a falloff near T_c which is sharper than BCS with $2\Delta(0) = 4.3kT_c$. The difference between mercury and lead lies mainly in the fact that the limiting cases are for $ql > 1$ and $ql < 1$, respectively, over the range $0 < T < T_c$.

In an attempt to reconcile these observations

with the X-band frequency measurements on thin polycrystalline mercury,[11] we have also undertaken in this work to test for the possible presence of dislocation damping contributions to the background ultrasonic attenuation. No dependence upon sound amplitude was observed over a dynamic range of up to 60 dB. Furthermore, a reasonable fit can be made to the free electron predicted dependence upon frequency and mean free path for the present experimental data. These tests, although not conclusive evidence against such mechanisms, at least indicate strongly that their influence is not likely to be large enough in magnitude to explain the observed anomalous behavior. Additional negative evidence relevant to the dislocation damping hypothesis is found in the Cd-doped Hg measurements of NS, which retain a non-BCS character even with a sharply reduced background attenuation, and presumably in a situation where there is extensive pinning of dislocations.

The experimental evidence accumulated to date for pure single-crystal mercury suggests that this strong coupling superconductor may deviate significantly from BCS predicted behavior. If the data are to be consistent with the BCS theory, vastly different multiple gaps are required, as well as a state-dependent electron mean free path. Additional experimental measurements in the difficult frequency range between 300 MHz and 9 GHz will be necessary to resolve the discrepancy between the results presented here and the X-band frequency results in polycrystalline mercury. The usefulness of further theoretical work perhaps is also indicated in view of the persistent anomalies which exist in the longitudinal ultrasonic measurements on mercury and lead.

ACKNOWLEDGMENTS

*Research sponsored by the Air Force Office of Scientific Research, Office of Aerospace Research, U. S. Air Force, under AFOSR Grant No. 68-1494A.

†Present address: Middlesex County College, Edison, N. J.

[1]R. L. Thomas, H. C. Wu, and N. Tepley, Phys. Rev. Letters 17, 22 (1966).

[2]J. Bardeen, L. N. Cooper, and J. Schrieffer, Phys. Rev. 108, 1175 (1957).

[3]C. P. Newcomb and R. W. Shaw, Phys. Rev. 173, 509 (1968).

[4]B. C. Deaton, Phys. Rev. Letters 16, 577 (1966).

[5]B. R. Tittmann and H. E. Bommel, Phys. Rev. 151, 178 (1966); 151, 189 (1966).

[6]W. A. Fate, Phys. Rev. 172, 402 (1968); W. A. Fate, R. W. Shaw, and G. L. Salinger, ibid., 413 (1968).

[7]L. T. Claiborne and N. G. Einsprunch, Phys. Rev. 151, 29 (1966).

[8]E. R. Dobbs and G. P. Thomas, in Proceedings of the Tenth International Conference on Low Temperature Physics, Moscow 1966, edited by M. P. Malkov (Proizvodstrenno-Izdatel'skii Kombinat, VINITI, Moscow, 1967), Vol. I.

[9]R. W. Morse, T. Olsen, and J. D. Gavenda, Phys. Rev. Letters 3, 15 (1959).

[10]J. M. Perz, Can. J. Phys. 44, 1765 (1966).

[11]R. B. Ferguson and J. H. Burgess, Phys. Rev. Letters 19, 494 (1967).

[12]W. P. Mason, Phys. Rev. 143, 229 (1966).

[13]A. B. Pippard, Proc. Roy. Soc. (London) A257, 165 (1960).

[14]T. Tsuneto, Phys. Rev. 121, 402 (1961).

[15]V. Ambegaokar and J. Woo, Phys. Rev. 139, A1818 (1965).

[16]V. Ambegaokar, Phys. Rev. Letters 16, 1047 (1966).

[17]J. W. F. Woo, Phys. Rev. 155, 429 (1967); 172, 423 (1968).

[18]H. V. Bohm, H. C. Wu, and N. Tepley, Mater. Res. Bull. 1, 13 (1966).

[19]R. W. Morse, in Progress in Cryogenics (Heywood, London, 1959), Vol. I, p. 230.

[20]G. C. Electronics, Rockford, Ill.

[21]G. N. Kammand and H. V. Bohm, Rev. Sci. Instr. 33, 957 (1962).

[22]J. B. Clement and E. H. Quinnell, Rev. Sci. Instr. 23, 5 (1952).

[23]B. Muhlschlegel, Z. Physik 155, 313 (1959).

[24]B. C. Deaton and J. D. Gavenda, Phys. Rev. 129, 1990 (1962).

[25]See, for example, B. Berre and T. Olsen, Phys. Status Solidi 11, 657 (1965).